



OPEN

Aging disrupts cell subpopulation dynamics and diminishes the function of mesenchymal stem cells

SUBJECT AREAS:

AGEING

REGENERATION

STEM-CELL RESEARCH

MECHANISMS OF DISEASE

Dominik Duscher^{1*}, Robert C. Rennert^{1*}, Michael Januszyk^{1,2*}, Ersilia Anghel¹, Zeshan N. Maan¹, Alexander J. Whittam¹, Marcelina G. Perez¹, Revanth Kosaraju¹, Michael S. Hu¹, Graham G. Walmsley¹, David Atashroo¹, Sacha Khong¹, Atul J. Butte^{2,3} & Geoffrey C. Gurtner¹

Received

15 August 2014

Accepted

28 October 2014

Published

21 November 2014

Correspondence and requests for materials should be addressed to G.C.G. (ggurtner@stanford.edu)

* These authors contributed equally to this work.

¹Hagey Laboratory for Pediatric Regenerative Medicine; Division of Plastic and Reconstructive Surgery, Department of Surgery, Stanford University School of Medicine, Stanford, CA, USA, ²Program in Biomedical Informatics, Stanford University School of Medicine, Stanford, CA, USA, ³Division of Systems Medicine, Department of Pediatrics, Stanford University School of Medicine, Stanford, CA, USA.

Advanced age is associated with an increased risk of vascular morbidity, attributable in part to impairments in new blood vessel formation. Mesenchymal stem cells (MSCs) have previously been shown to play an important role in neovascularization and deficiencies in these cells have been described in aged patients. Here we utilize single cell transcriptional analysis to determine the effect of aging on MSC population dynamics. We identify an age-related depletion of a subpopulation of MSCs characterized by a pro-vascular transcriptional profile. Supporting this finding, we demonstrate that aged MSCs are also significantly compromised in their ability to support vascular network formation *in vitro* and *in vivo*. Finally, aged MSCs are unable to rescue age-associated impairments in cutaneous wound healing. Taken together, these data suggest that age-related changes in MSC population dynamics result in impaired therapeutic potential of aged progenitor cells. These findings have critical implications for therapeutic cell source decisions (autologous versus allogeneic) and indicate the necessity of strategies to improve functionality of aged MSCs.

The United States is facing a rapid increase in its elderly population. According to U.S. Census Bureau projections, the number of Americans age sixty-five and older is expected to more than double between 2012 and 2060¹. Concomitant with an aging population is an increased risk for vasculopathies, including cardiovascular disease, peripheral vascular disease, and impaired wound healing^{2,3}. One of the main underlying causes for this is an impairment of new blood vessel formation, or neovascularization^{4,5}. Progenitor cell populations, such as mesenchymal stem cells (MSCs), have been shown to promote neovascularization following therapeutic application through the secretion of pro-vascular cytokines^{6,7}.

Unfortunately, aging is known to have a negative impact on the regenerative capacities of most tissues⁸, and recent evidence suggests that stem cells are also susceptible to biologic aging^{9,10}. Aged MSCs in particular have been shown to possess impairments in proliferation and differentiation capacity^{9–11}, as well as alterations in therapeutic gene expression and cytokine production^{12,13}. However, the mechanisms underlying control of the aging process in human cells remain poorly understood¹⁴, limiting the development of cell based therapies.

Only in the last few years have high-resolution measurement tools evolved to interrogate heterogeneous cell populations like mesenchymal progenitors with sufficient precision to detect potentially subtle population shifts¹⁵. Our laboratory has recently developed a novel method that combines high throughput single cell gene expression analysis with complex mathematical modeling to identify critical perturbations in cell subpopulations¹⁶. Applying this approach to study diabetes, a condition also associated with a global breakdown of reparative processes, we identified critical disruptions in “progenitor cell ecology” which were responsible for impairments in the formation of new blood vessels in response to ischemia (neovascularization)^{17,18}. Given that aging is likewise associated with significant neovascular impairments^{19,4}, and that vascular disease is the leading cause of death in the aged population²⁰, we sought to evaluate the cellular dynamics of aging in this context.

Wound healing is a common and easily measured indicator of impaired neovascularization and is clinically impaired in aging²¹. Progenitor cell-based therapy using allogeneic or autologous cells applied to the wound site

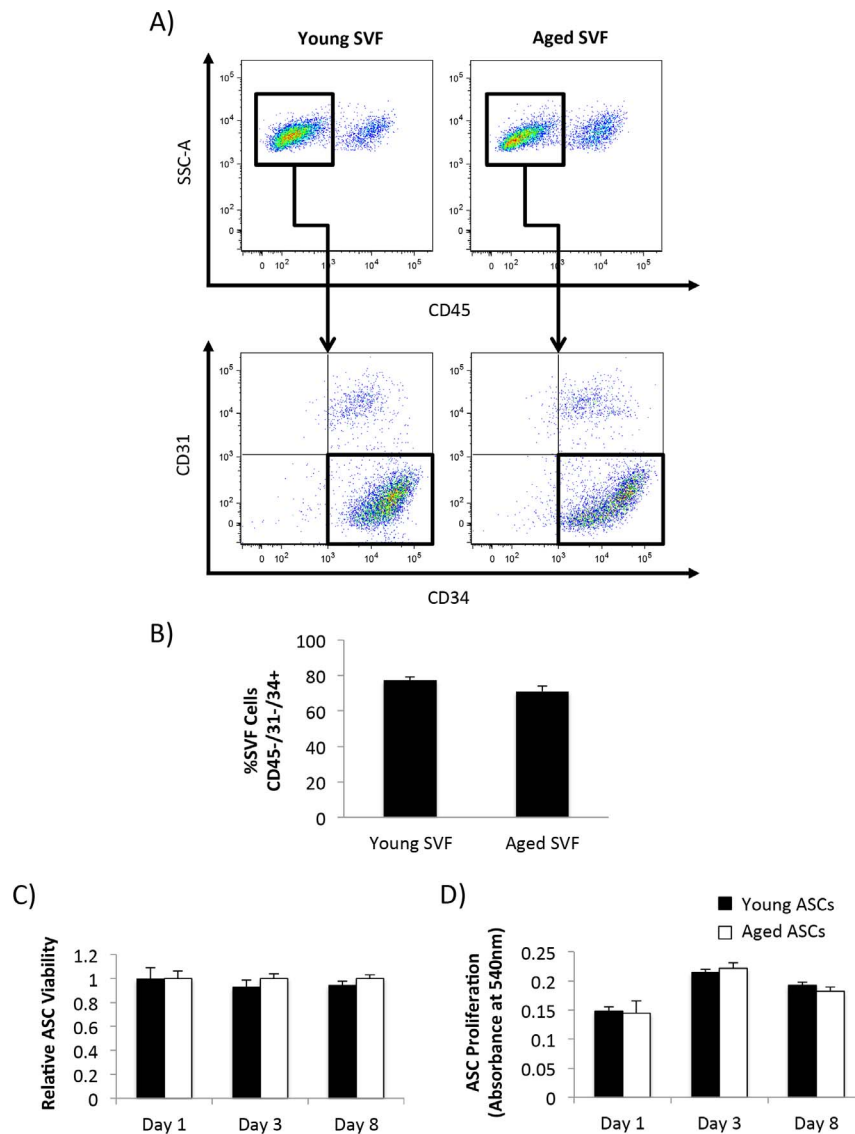


Figure 1 | Assessment of age on ASC phenotype. (A) Flow cytometric analysis determining the % of CD45⁻ cells (top row) and ASCs (CD45⁻/31⁻/34⁺ cells; bottom row) within the SVF of young and aged mice. (B) Quantification of CD45⁻/31⁻/34⁺ ASCs in young and aged SVF reveals no significant difference in ASC frequency across samples. (C,D) Live/dead and MTT proliferation assays revealed no significant differences in the viability or proliferation of young and aged ASCs following *in vitro* hydrogel seeding.

represent an attractive strategy to treat impaired wound healing in advanced age. Here we evaluate the direct effect of aging on MSC functionality, specifically determining the ability of these cells to support vascular network formation *in vitro* and *in vivo*. Building on previous work demonstrating that MSCs accelerate wound vascularization and closure^{6,7}, we also sought to determine whether the delivery of aged MSCs would similarly improve wound healing, or whether these cells were impaired and thus limited in their potential clinical effectiveness.

Results

Aging does not influence MSC frequency, viability, or proliferative capacity. We first assessed whether aging affected the MSC phenotype. Consistent with previous studies^{22,23}, the frequency of MSCs within adipose tissue (as determined by the percentage of CD45⁻/CD31⁻/CD34⁺ cells within the SVF) was unaffected by age (Figure 1A–B). Furthermore, aging had no effect on adipose derived mesenchymal stem cell (ASC) viability and proliferation following hydrogel seeding *in vitro* (Figure 1C–D). Because these population-level phenotypic similarities did not explain the signaling and

functional deficiencies associated with aged progenitor cells¹³, we next analyzed ASC subpopulation dynamics via single cell interrogation of young and aged cells.

Aging selectively depletes a putatively vasculogenic cell subpopulation.

Utilizing a previously described microfluidic-based single-cell gene expression platform¹⁶, the transcriptional profiles of 75 individual cells per group were simultaneously evaluated for approximately 70 gene targets related to stemness, vasculogenesis, and tissue regeneration (Supplemental Table 1). In this analysis, ASCs isolated from both young and aged mice displayed significant heterogeneity at the single-cell level (Figure 2A–B). Differences in the transcriptional profiles of genes related to cell stemness, vasculogenesis, and tissue remodeling, such as the metalloproteinase *Adam10*, the chemokines *Angpt1* and *2*, and the transcription factors *Hif1a* and *Mef2c*^{24–28}, were also observed (Figure 2C). Additionally, Kolmogorov-Smirnov analysis of these single-cell data confirmed differential expression of the anti-oxidative enzyme *Sod2* in aged versus young ASCs ($p < 0.01$).

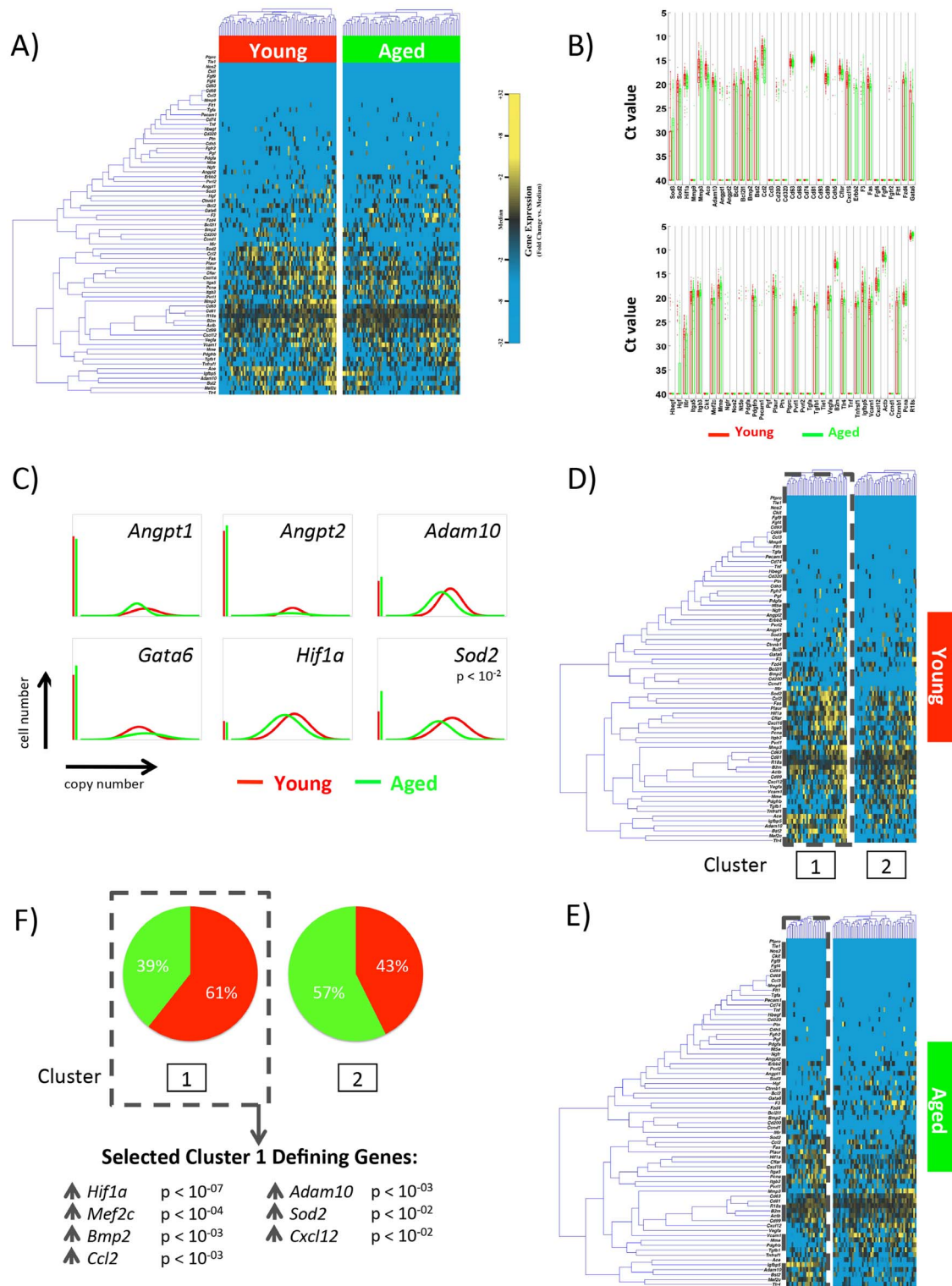


Figure 2 | Single cell transcriptional analysis of young and aged ASCs. (A) Hierarchical clustering of cells from young (left) and aged (right) mice. Gene expression is presented as fold change from median on a color scale from yellow (high expression, 32-fold above median) to blue (low expression, 32-fold below median). (B) Whisker plots presenting raw qPCR cycle threshold values for each gene across all young and aged ASCs. Individual dots represent single gene/cell qPCR reactions, with increased cycle threshold values corresponding to decreased mRNA content. Cycle threshold values of 40 were assigned to all reactions that failed to achieve detectable levels of amplification within 40 qPCR cycles. (C) Median-centered Gaussian fit curves of selected genes relating to cell stemness and vasculogenesis displaying grossly differential expression profiles between young and aged cells. Non-parametric two-sample Kolmogorov-Smirnov analysis confirmed the differential expression of the anti-oxidative enzyme *Sod2* in aged versus young ASCs ($p < 0.01$). The left bar represents the fraction of qPCR reactions that failed to amplify in each group. (D,E) Partitional clustering of young and aged cells based on the expression patterns of all 71 genes ($k = 2$). (F) Pie charts representing the fraction of ASCs comprising each cluster (Young [red], Aged [green]), with selected cluster 1-defining genes listed below.

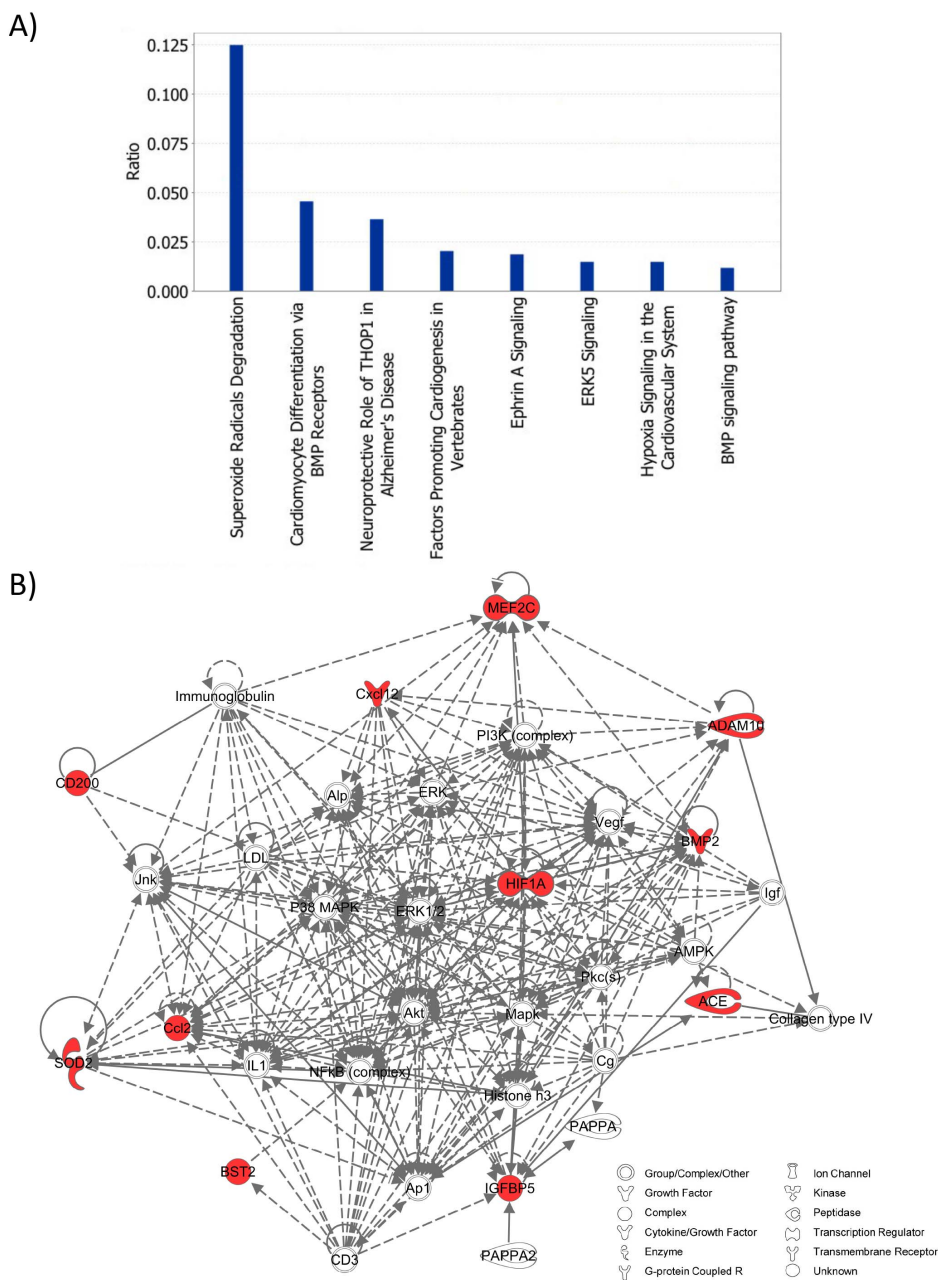


Figure 3 | Pathway analysis of a pro-vascular ASC subpopulation. (A) Canonical pathways enriched for genes whose expression was significantly increased in cells comprising Cluster 1 in Figure 2C–D. (B) Top scoring Ingenuity Pathway Analysis (IPA)-constructed transcriptome network based on genes that were significantly increased in Cluster 1 cells. These significant “seed” genes are colored in red to distinguish them from the remaining “inferred” entities in the network.

To further examine this niche, the super-set of transcriptional profiles of aged and young cells was subjected to a partitioning clustering algorithm¹⁶. This analysis identified two distinct transcriptionally defined ASC clusters in each group, with the first cluster possessing considerably fewer aged cells (Figure 2D–F). Critically, this subpopulation was characterized in part by the increased expression of genes associated with stemness, tissue remodeling, and vasculogenesis, such as *Mef2c*, *Hif1a*, *Adam10*, *Ccl2*, and *Cxcl12*^{24–26,29,30} (Figure 2F, Supplemental Table 2), suggesting it may represent a more pluripotent subset of this heterogeneous cell collection.

Canonical pathways whose expression was significantly upregulated in this cluster were determined using Ingenuity Pathway Analysis (IPA). These included multiple cardiovascular processes, including development, differentiation, and hypoxic signaling, as

well as the degradation of superoxide radicals, lending additional support to a pro-vasculogenic role for these cells (Figure 3A). Furthermore, the top molecular network associated with these genes based on the Ingenuity Knowledge Base appears to link key mediators of neovascularization (*Hif1a*, *VEGF*, and *CXCL12*)^{31,32} and wound healing (*Ccl2*, *P38*, *MAPK*, and *IL1*)^{33–36} (Figure 3B). Collectively, these data support the depletion of a putatively vasculogenic subpopulation of ASCs as a potential mechanism underlying age-related impairments in ASC regenerative potential, particularly in the context of ischemic wound healing.

Aging disrupts MSC signaling and angiogenic potential. To investigate whether the subpopulation differences discovered at the single cell level were artificial, we assessed the effect of age on the ASC *in situ* environment. Consistent with an age-related signaling

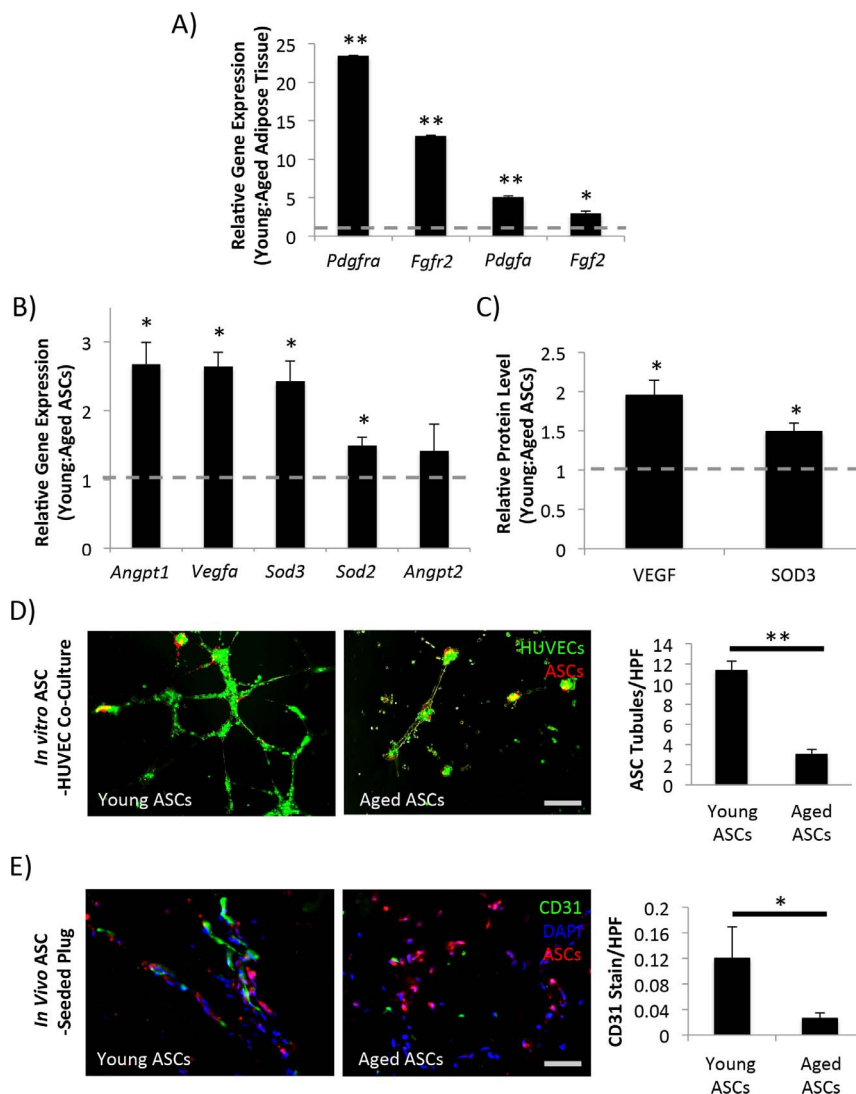


Figure 4 | Analysis of ASC neovascular potential. (A) Transcriptional profiles of murine fat pads exhibit dysfunctional *in situ* signaling in aged samples. (B–C) RT-PCR and ELISA quantifying the relative expression of selected vasculogenic and anti-oxidant genes in young versus aged ASCs *in vitro*. (D) Matrigel co-culture of ASCs and HUVECs under hypoxic conditions *in vitro*. (E) *In vivo* aged and young ASC-seeded matrigel plugs harvested on day twelve stained for the endothelial cell marker CD31. Scale bar = 25 μ m. ** indicates $p \leq 0.01$; * indicates $p \leq 0.05$.

dysfunction in this setting, the expression of multiple growth factors (*Fgf2*, *Pdgfa*, $p < 0.05$), as well as their receptors (*Fgfr2*, *Pdgfra*, $p < 0.01$), was diminished in aged adipose tissue (Figure 4A). Similar negative effects on paracrine signaling could be detected in isolated aged ASCs seeded within hydrogel bioscaffolds *in vitro*. Specifically, aged ASCs displayed decreased transcriptional expression and production of several vasculogenesis-related and anti-oxidative molecules, such as *Angpt1*, *Vegfa*, and *Sod3* ($p < 0.05$) (Figure 4B–C).

Given the significant signaling disruption observed in aged samples, we next sought to directly examine the potential of aged ASCs to support vasculogenesis via cytokine signaling *in vitro* and *in vivo*. To analyze the ability of ASCs to promote endothelial cell sprouting (an *in vitro* surrogate for vascular formation), aged and young ASCs were co-cultured with HUVEC cells on matrigel under hypoxic conditions. Indicative of a reduced cytokine stimulatory capacity with aging, young ASCs supported significantly greater HUVEC tubule formation than their aged counterparts (11.4 vs. 3.1 tubules/HPF, $p < 0.01$) (Figure 4D).

To confirm that the *in vitro* vasculogenic impairments in aged ASCs were also present *in vivo*, a matrigel plug vascularization assay was performed³⁷. Interestingly, while ASC survival was not signifi-

cantly different across groups (Supplemental Figure 1), consistent with our *in vitro* findings plugs containing aged ASCs were significantly less vascularized (0.02 vs 0.12% CD31 staining/HPF, $p < 0.05$) (Figure 4E). Together, these data demonstrate that aging significantly impairs the potential of ASCs to promote neovascularization both *in vitro* and *in vivo*.

Aged MSCs are unable to improve cutaneous wound healing in aged mice. To evaluate the translational potential of autologous aged ASCs for the promotion of wound healing, cell-seeded hydrogels were applied to aged murine excisional cutaneous wounds utilizing a previously established model³⁸. While wounds treated with young ASC-seeded hydrogels showed significantly improved healing rates as early as day six (Figure 5A–B), and resulted in significantly faster wound closure times as compared to controls (14.0 vs 15.8 days, $p < 0.05$), aged ASCs failed to enhance wound healing rates (Figure 5B) or closure times (15.4 vs. 15.8 days, $p = 0.89$) (Figure 5C).

Aged MSCs fail to enhance wound vascularity or modulate wound anti-oxidative or vasculogenic profiles. To better characterize the therapeutic dysfunction of aged ASCs *in vivo*, immunohistochemical

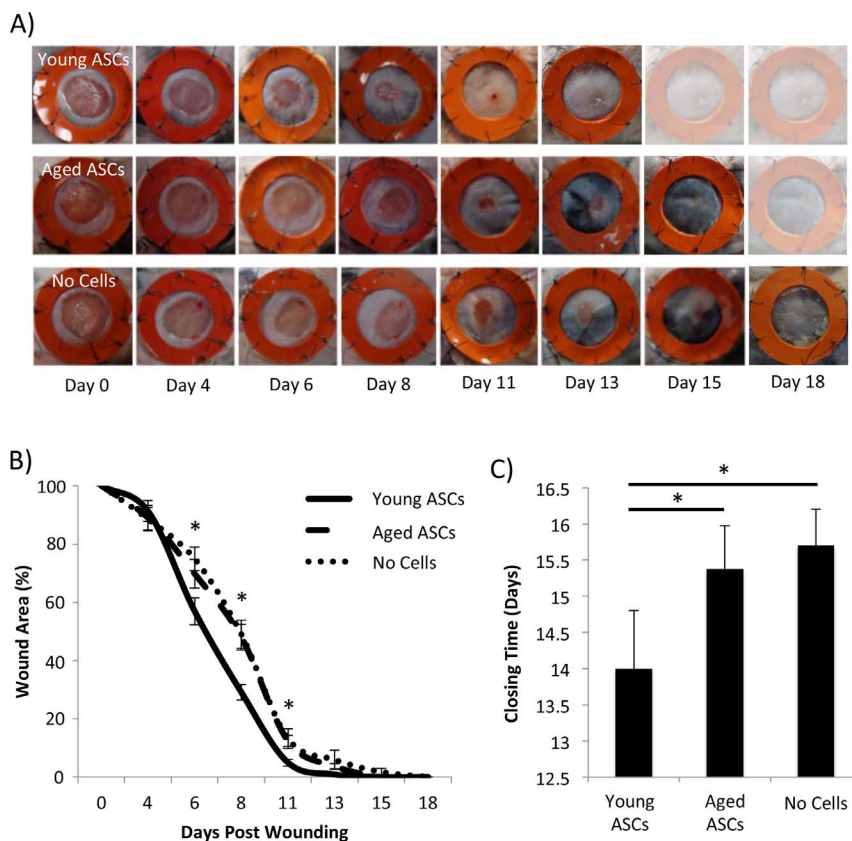


Figure 5 | Application of young but not aged ASCs improves excisional wound healing. (A,B) Gross appearance and area measurements of humanized excisional murine wounds treated with aged and young ASCs. Application of young ASCs resulted in accelerated wound healing from day six on compared to wounds treated with aged ASCs or no cells. (C) Application of young ASCs resulted in an accelerated time to wound closure compared to wounds treated with aged ASCs or no cells. * indicates $p \leq 0.05$.

staining of day four wounds was performed for the anti-oxidative and pro-vasculogenic molecules SOD-3 and VEGF. Diminished levels of both SOD-3 (Figure 6A) and VEGF (Figure 6B) were found in wounds treated with aged versus young ASCs, with the aged cells displaying a therapeutic efficacy similar to that of the no cell control. Consistent with this signaling dysfunction, healed wounds in the aged ASC treatment group displayed significantly less neovascularization (0.15 vs. 0.52% CD31 staining/HPF, $p < 0.01$) (Figure 6C), with the aged ASC group again showing no significant increase over acellular controls. These data further underscore the significance of the impaired regenerative potential of aged ASCs *in vivo*.

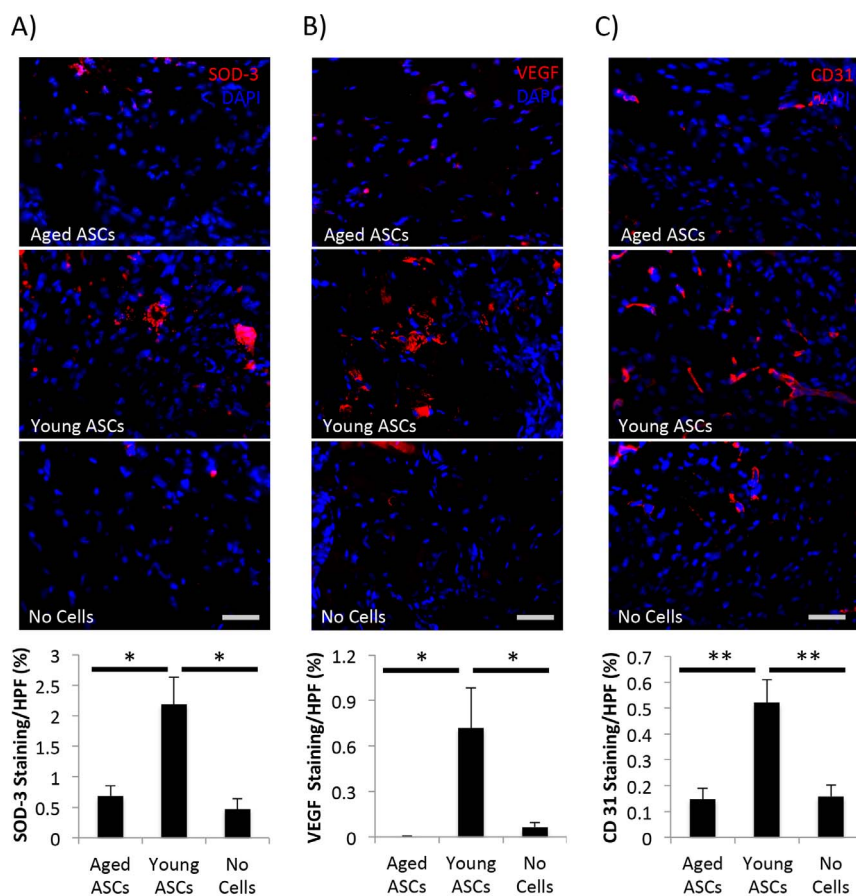
Discussion

In this study, we identified age-related alterations in MSC subpopulation dynamics at a single cell level that may explain the reduced vasculogenic potential of aged MSCs. These findings are congruent with the concept that complex cell populations such as progenitor cells are characterized by a level of functional heterogeneity that may be critical to their biological role, and that the selective loss of different functional cell populations and thereby complexity may be one of the fundamental mechanisms of aging. This idea is supported by some theoretical work in the aging literature^{39,40} as well as evidence that certain stem/progenitor cell populations disappear during the aging process^{41–50}.

Studying the effects of aging on progenitor cell populations is difficult, however, as traditional population-level approaches rely on pooled RNA or protein from hundreds of thousands of cells, and are thus unable to detect differential expression among rare cells and/or subgroups. Only recently have high-throughput techniques

evolved to interrogate samples with single cell resolution. These systems make use of microfluidic technology to achieve massively parallel single-cell gene expression analysis, the resulting data from which can provide novel insights into the relationships among cells in complex tissues^{51–53}. Our laboratory has developed a novel method that combines single cell transcriptional analysis with advanced mathematical modeling to characterize heterogeneity in putatively homogeneous populations, as well as identify critical perturbations in cell subpopulations (cellular ecology) under pathologic conditions^{16,54–57}. Utilizing this methodology, we have previously demonstrated that impaired neovascularization is linked to selective depletion of progenitor cell populations in diabetes, a disease associated with many of the same vasculopathies found in aging^{17,18}. By evaluating whether a similar disruption in progenitor cell populations is associated with impaired neovascularization in advanced age, we set out to determine the clinical potential of this cell source, as well as provide fundamental insights into the effect of aging on progenitor cells.

Highlighting the value of this approach, age did not have an effect on ASC frequency or population-level phenotype that would explain their reduced vasculogenic potential^{12,13}. This finding is consistent with previous reports of ASC cell-surface markers remaining intact with aging⁵⁸. Conversely, high-resolution transcriptional analysis identified age-related differences in key genes involved in ischemic neovascularization, including the hypoxic transcription factor *Hif1a* and chemokine *Cxcl12* (*Sdf1*), as well as the anti-oxidative enzyme *Sod2*. When subjected to partitioned clustering, aged animals also had significantly fewer cells in the subcluster defined by vasculogenesis-related genes, such as *Cxcl12*, *Hif1a*, *Sod2*, and *Ccl2*. These results suggest that deficits in the neovascular potential of aged progenitor cells may be the result of selective subpopulation depletion.



Consistent with these single-cell data, we found that while young ASCs improved wound healing in aged mice, this effect was absent when using ASCs isolated from aged mice. Mechanistically, this decrease in ASC *in vivo* therapeutic efficacy was likely due to the depletion of a functional subset of ASCs expressing anti-oxidative and pro-regenerative cytokines, as multiple pro-regenerative pathways within the wound that were upregulated with application of young ASCs were not affected following application of aged cells. These data support a decrease in progenitor cell heterogeneity and removal of critical cell subsets as potential key factors leading to the loss of cellular complexity and tissue homeostasis in aging, which would have considerable implications for new diagnostic and therapeutic approaches in this population. Specifically, adding back the depleted cellular subpopulations (as was done with the utilization of young cells in this work) may be an effective strategy to combat not only impaired wound healing, but also other age related sequelae.

Taken together, these findings demonstrate that MSCs are susceptible to biological aging that results in impairments in their regenerative capacity. Single-cell transcriptional interrogation of these cells suggests that depletion of a pro-vasculogenic subpopulation may underlie many of the well-known consequences of aging such as neovascular dysfunction. Given the significant healthcare burden associated with age-related morbidity, and the limitations in current therapeutic approaches grounded in existing theories of aging^{59,60}, this more quantitative understanding of how aging causes progenitor cell dysfunction suggests the need for novel therapeutic and diagnostic tools addressing age-associated impairments in cellular heterogeneity.

Methods

Animals. Young (3 months) and aged (21 months) wild-type (WT, C57BL/6) mice were obtained from the National Institute on Aging (NIA, Bethesda, MD). All protocols were approved by the Stanford Administrative Panel on Laboratory Animal Care and all experiments were performed in accordance with relevant guidelines and regulations.

ASC *in situ* analysis. Young and aged murine inguinal fat pads were harvested and manually disrupted for real-time quantitative PCR (RT-PCR) as described below.

ASC harvest and culture. ASCs were isolated from young and aged murine inguinal fat pads, minced and digested for one hour at 37°C using collagenase I (Roche Applied Science, Indianapolis, IN). After centrifugation, the pelleted stromal vascular fraction (SVF) was cultured in supplemented DMEM. Cells were used at or before passage two, and all analyses were run in triplicate unless otherwise stated.

***In vitro* HUVEC matrigel tubulization assay.** 2×10^4 PKH26-labeled young or aged ASCs were mixed with 2×10^5 calcein-labeled human umbilical vein endothelial cells (HUVECs) (Life Technologies, Grand Island, NY) and cultured for 12 hours under hypoxic conditions on a 24-well plate coated with growth factor reduced Matrigel (BD Biosciences, Franklin Lakes, NJ). HUVEC tubule counts were determined in 5 random high-power fields per well using an inverted Leica DMIL microscope.

***In vivo* matrigel plug assay.** 8×10^5 PKH26-labeled young or aged ASCs were suspended in 250 μ l of growth factor reduced Matrigel (BD Biosciences) and injected in a subcutaneous fashion on the dorsum of 8-12 week old WT mice. Plugs were harvested at day 12, embedded in OCT (Sakura Finetek USA, Inc., Torrance CA), sectioned, and immunohistochemically stained for CD31 as described below. ASC cell density was determined based on cell counts per high power field.

***In vitro* hydrogel bioscaffold seeding.** 1×10^5 ASCs were suspended in 15 μ l of growth media and seeded within a 5% collagen-pullulan hydrogel bioscaffold as previously described⁶⁷. Seeded scaffolds were placed in growth media and incubated



at 37°C in 5% CO₂ prior to proliferation and survival analyses, or RNA/protein harvest.

In vitro viability and proliferation. A live-dead assay was performed to assess ASC viability at days 1, 3 and 8 following hydrogel seeding, according to manufacturer's instructions (Live/Dead Cell Viability Assay, Life Technologies, Grand Island, NY). ASC proliferation was assessed at days 1, 3 and 8 following hydrogel seeding using an MTT assay (Vybrant MTT Cell Proliferation Assay Kit, Invitrogen, Grand Island, NY).

Real-time quantitative PCR (RT-PCR). Total RNA was isolated from ground fat pads or plated/hydrogel-seeded ASCs using the RNeasy Mini Kit (Qiagen, Germantown, MD) and transcribed to cDNA (Superscript First-Strand Synthesis Kit, Invitrogen, Grand Island, NY). Real-time qPCR reactions were performed using Taqman gene expression assays (Applied Biosystems, Foster City, CA) for murine *Angpt1* (Angiopoietin 1, Mm00456503_m1), *Vegfa* (Vascular endothelial growth factor-A, Mm01281447_m1), *Sod3* (Superoxide dismutase 3, Mm01213380_s1), *Sod2* (Superoxide dismutase 2, Mm00449726_m1), *Angpt2* (Angiopoietin 2, Mm00545822), *Fgf2* (Fibroblast growth factor 2, Mm00433287_m1), *Fgfr2* (Fibroblast growth factor receptor 2, Mm01269930_m1), *Pdgfra* (Platelet derived growth factor-A, Mm01205760_m1) and *Pdgfra* (Platelet derived growth factor receptor-A, Mm01205760_m1) using a Prism 7900HT Sequence Detection System (Applied Biosystems). Expression levels of the target genes were normalized to *Actb* (Beta actin, Mm01205647_g1) or *B2m* (Beta-2-microglobulin, Mm00437764_m1). See supplemental table 3 for overview.

In vitro cytokine quantification. Total protein was collected from ASC-seeded hydrogels using RIPA buffer (Sigma-Aldrich) in combination with a protease inhibitor. Protein levels of VEGF and SOD3 were quantified using murine ELISA kits (R&D Systems, Minneapolis, MN and USCN, Wuhan, China).

In vivo excisional wound model. Twenty-one month old male C57Bl/6 mice were randomized into three treatment groups: young or aged murine ASC-seeded hydrogel and unseeded hydrogel control (n=5 per group). As previously described³⁸, two 6 mm full-thickness cutaneous wounds were excised on either side of the midline, with each wound stented with silicone rings sutured in place to prevent wound contraction. For mice in the unseeded hydrogel group, a 6 mm piece of hydrogel saturated with PBS was placed in each wound bed. For mice in the ASC-seeded hydrogel groups, a 6 mm piece of hydrogel seeded with 2×10^5 young or aged ASCs was placed in the wound bed following creation. All wounds were covered with an occlusive dressing (Tegaderm, 3M, St. Paul, MN). Digital photographs were taken on day 0, 4, 6, 8, 11, 13, 15 and 18. Wound area was measured using Image J software (NIH, Bethesda, MD).

Immunohistochemistry (IHC). Wounds from the excisional model were harvested upon closure and immediately embedded in OCT (Sakura Finetek USA, Inc.). To assess vasculature in healed wounds and matrigel plug samples, seven micron thick frozen sections were immunohistochemically stained for CD31 (1° - 1:100 Rb α CD31, Ab28364, Abcam, 2° - 1:400 AF547 or AF488 Gt α Rb, Life Technologies). To assess *in vivo* signaling during wound healing, day four wounds from a separate cohort of mice were similarly harvested and subjected to immunohistochemical staining for SOD3 (1° - 1:100 Rb α SOD3, Ab21974, Abcam; 2° - 1:200 AF547 Gt α Rb, Life Technologies) and VEGF (1° - 1:100 Rb α VEGF, Ab1316, Abcam, Cambridge, MA; 2° - 1:200 AF547 Gt α Rb, Life Technologies). For all IHC analyses, nuclei were stained with DAPI, and Image J (NIH) was used to binarize images taken with the same settings. Intensity thresholds were used to quantify CD31 staining based upon pixel-positive area per high power field.

Microfluidic single-cell gene expression analysis. Young and aged primary ASCs with the surface marker profile CD45⁻/CD31⁺/CD34⁺ (to exclude contaminating hematopoietic and endothelial cells found within the SVF) were sorted as single cells using a Becton Dickinson FACSAria flow cytometer into 6 μ l of lysis buffer. Reverse transcription and low cycle pre-amplification were performed using Cells Direct (Invitrogen) with Taqman assay primer sets (Applied Biosystems) as per the manufacturers specifications. cDNA was loaded onto 96.96 Dynamic Arrays (Fluidigm, South San Francisco, CA) for qPCR amplification using Universal PCR Master Mix (Applied Biosystems) with a uniquely compiled Taqman assay primer set as previously described⁵⁵.

Statistical analysis. Results are presented as mean \pm standard error of the mean (SEM). Data analysis was performed using a Student's t-test. Results were considered significant for $p \leq 0.05$. For the single cell gene expression analysis, a two sample Kolmogorov-Smirnov (K-S) test was used to compare empirical distributions, using a strict cutoff of $p < 0.01$ following Bonferroni correction for multiple samples. Transcriptionally defined subpopulations were determined using an adaptive fuzzy c-means clustering algorithm employing a standard Euclidean distance metric, as previously described⁵⁵. Each cell was assigned partial membership to each cluster based on similarities in expression profiles, with optimally partitioned clusters flattened and sub-grouped using hierarchical clustering in order to facilitate visualization of data patterning within and across these clusters. Canonical pathway calculations and network analyses were performed using Ingenuity Pathway Analysis

(IPA, Ingenuity Systems, Redwood City, CA) based on genes differentially expressed among cell subpopulations.

1. U.S. Census Bureau, Projections Show a Slower Growing, Older, More Diverse Nation a Half Century from Now, <https://www.census.gov/newsroom/releases/archives/population/cb12-243.html>, (2012). (Date of access: 04/10/2014).
2. Reed, M. J. & Edelberg, J. M. Impaired angiogenesis in the aged. *Sci Aging Knowledge Environ* : SAGE KE **2004**, pe7, doi:10.1126/sageke.2004.7.pe7 (2004).
3. Guo, S. & Dipietro, L. A. Factors affecting wound healing. *J Dent Res* **89**, 219–229, doi:10.1177/0022034509359125 (2010).
4. Chang, E. I. *et al.* Age decreases endothelial progenitor cell recruitment through decreases in hypoxia-inducible factor 1 α stabilization during ischemia. *Circulation* **116**, 2818–2829, doi:10.1161/CIRCULATIONAHA.107.715847 (2007).
5. Felice, F., Barsotti, M. C., Poredos, P., Balbarini, A. & Di Stefano, R. Effect of aging on metabolic pathways in endothelial progenitor cells. *Curr Pharm Des* **19**, 2351–2365 (2013).
6. Garg, R. K. *et al.* Capillary Force Seeding of Hydrogels for Adipose-Derived Stem Cell Delivery in Wounds. *Stem Cells Trans Med* **3**, 1079–89. doi:10.5966/sctm.2014-0007 (2014).
7. Rustad, K. C. *et al.* Enhancement of mesenchymal stem cell angiogenic capacity and stemness by a biomimetic hydrogel scaffold. *Biomaterials* **33**, 80–90, doi:10.1016/j.biomaterials.2011.09.041 (2012).
8. Troen, B. R. The biology of aging. *Mount Sinai J Med* **70**, 3–22 (2003).
9. Wu, W., Niklason, L. & Steinbacher, D. M. The effect of age on human adipose-derived stem cells. *Plast Reconstr Surg* **131**, 27–37, doi:10.1097/PRS.0b013e3182729cfc (2013).
10. Alt, E. U. *et al.* Aging alters tissue resident mesenchymal stem cell properties. *Stem Cell Res* **8**, 215–225, doi:10.1016/j.scr.2011.11.002 (2012).
11. Madonna, R. *et al.* Age-dependent impairment of number and angiogenic potential of adipose tissue-derived progenitor cells. *Eur J Clin Invest* **41**, 126–133, doi:10.1111/j.1365-2362.2010.02384.x (2011).
12. Efimenko, A., Starostina, E., Kalinina, N. & Stolzing, A. Angiogenic properties of aged adipose derived mesenchymal stem cells after hypoxic conditioning. *J Trans Med* **9**, 10, doi:10.1186/1479-5876-9-10 (2011).
13. De Barros, S. *et al.* Aging-related decrease of human ASC angiogenic potential is reversed by hypoxia preconditioning through ROS production. *Mol Ther* **21**, 399–408, doi:10.1038/mt.2012.213 (2013).
14. Jin, K. Modern Biological Theories of Aging. *Aging Dis* **1**, 72–74 (2010).
15. Januszyk, M. & Gurtner, G. C. High-Throughput Single-Cell Analysis for Wound Healing Applications. *Adv Wound Care (New Rochelle)* **2**, 457–469, doi:10.1089/wound.2012.0395 (2013).
16. Glotzbach, J. P. *et al.* An information theoretic, microfluidic-based single cell analysis permits identification of subpopulations among putatively homogeneous stem cells. *PLoS One* **6**, e21211, doi:10.1371/journal.pone.0021211 (2011).
17. Rennert, R. C. *et al.* Diabetes impairs the angiogenic potential of adipose derived stem cells by selectively depleting cellular subpopulations. *Stem Cell Res Ther* **5**, 79, doi:10.1186/srct468 (2014).
18. Januszyk, M. *et al.* Diabetes Irreversibly Depletes Bone Marrow-Derived Mesenchymal Progenitor Cell Subpopulations. *Diabetes* **9**, 3047–56, doi:10.2337/db13-1366 (2014).
19. Hoenig, M. R., Bianchi, C., Rosenzweig, A. & Sellke, F. W. Decreased vascular repair and neovascularization with ageing: mechanisms and clinical relevance with an emphasis on hypoxia-inducible factor-1. *Curr Mol Med* **8**, 754–767 (2008).
20. Go, A. S. *et al.* Heart disease and stroke statistics--2013 update: a report from the American Heart Association. *Circulation* **127**, e6–e245, doi:10.1161/CIR.0b013e31828124ad (2013).
21. Bauer, S. M., Bauer, R. J. & Velazquez, O. C. Angiogenesis, vasculogenesis, and induction of healing in chronic wounds. *Vasc Endovascular Surg* **39**, 293–306 (2005).
22. Aust, L. *et al.* Yield of human adipose-derived adult stem cells from liposuction aspirates. *Cytotherapy* **6**, 7–14, doi:10.1080/14653240310004539 (2004).
23. Jurgens, W. J. *et al.* Effect of tissue-harvesting site on yield of stem cells derived from adipose tissue: implications for cell-based therapies. *Cell Tissue Res* **332**, 415–426, doi:10.1007/s00441-007-0555-7 (2008).
24. Pothoff, M. J. & Olson, E. N. MEF2: a central regulator of diverse developmental programs. *Development* **134**, 4131–4140, doi:10.1242/dev.008367 (2007).
25. van Hinsbergh, V. W. & Koolwijk, P. Endothelial sprouting and angiogenesis: matrix metalloproteinases in the lead. *Cardiovasc Res* **78**, 203–212, doi:10.1093/cvr/cvm102 (2008).
26. Razban, V. *et al.* HIF-1 α Overexpression Induces Angiogenesis in Mesenchymal Stem Cells. *Biores Open Access* **1**, 174–183, doi:10.1089/biores.2012.9905 (2012).
27. Babaei, S. *et al.* Angiogenic actions of angiopoietin-1 require endothelium-derived nitric oxide. *Am J Pathol* **162**, 1927–1936, doi:10.1016/S0002-9440(10)64326-X (2003).
28. Felcht, M. *et al.* Angiopoietin-2 differentially regulates angiogenesis through TIE2 and integrin signaling. *J Clin Invest* **122**, 1991–2005, doi:10.1172/JCI58832 (2012).



29. Deshane, J. *et al.* Stromal cell-derived factor 1 promotes angiogenesis via a heme oxygenase 1-dependent mechanism. *J Exp Med* **204**, 605–618, doi:10.1084/jem.20061609 (2007).
30. Stamatovic, S. M., Keep, R. F., Mostarica-Stojkovic, M. & Andjelkovic, A. V. CCL2 regulates angiogenesis via activation of Ets-1 transcription factor. *J Immunol* **177**, 2651–2661 (2006).
31. Loh, S. A. *et al.* SDF-1 alpha expression during wound healing in the aged is HIF dependent. *Plast Reconstr Surg* **123**, 65S–75S, doi:10.1097/PRS.0b013e318191bdf4 (2009).
32. Thangarajah, H. *et al.* The molecular basis for impaired hypoxia-induced VEGF expression in diabetic tissues. *Proc Natl Acad Sci U S A* **106**, 13505–13510, doi:10.1073/pnas.0906670106 (2009).
33. Wood, S. *et al.* Pro-Inflammatory Chemokine CCL2 (MCP-1) Promotes Healing in Diabetic Wounds by Restoring the Macrophage Response. *PLoS One* **9**, e91574, doi:10.1371/journal.pone.0091574 (2014).
34. Yew, T. L. *et al.* Enhancement of wound healing by human multipotent stromal cell conditioned medium: the paracrine factors and p38 MAPK activation. *Cell Transplant* **20**, 693–706, doi:10.3727/096368910X550198 (2011).
35. Wood, L. C. *et al.* Barrier disruption stimulates interleukin-1 alpha expression and release from a pre-formed pool in murine epidermis. *J Invest Dermatol* **106**, 397–403 (1996).
36. Barrientos, S., Stojadinovic, O., Golinko, M. S., Brem, H. & Tomic-Canic, M. Growth factors and cytokines in wound healing. *Wound Repair Regen* **16**, 585–601, doi:10.1111/j.1524-475X.2008.00410.x (2008).
37. Malinda, K. M. In vivo matrigel migration and angiogenesis assay. *Methods in molecular biology* **467**, 287–294, doi:10.1007/978-1-59745-241-0_17 (2009).
38. Galiano, R. D., Michaels, J. T., Dobryansky, M., Levine, J. P. & Gurtner, G. C. Quantitative and reproducible murine model of excisional wound healing. *Wound Repair Regen* **12**, 485–492, doi:10.1111/j.1067-1927.2004.12404.x (2004).
39. Lipsitz, L. A. & Goldberger, A. L. Loss of ‘complexity’ and aging. Potential applications of fractals and chaos theory to senescence. *Jama* **267**, 1806–1809 (1992).
40. Manor, B. & Lipsitz, L. A. Physiologic complexity and aging: implications for physical function and rehabilitation. *Prog Neuropsychopharmacol Biol Psychiatry* **45**, 287–293, doi:10.1016/j.pnpb.2012.08.020 (2013).
41. Senitz, D., Reichenbach, A. & Smith, T. G., Jr. Surface complexity of human neocortical astrocytic cells: changes with development, aging, and dementia. *J Hirnforsch* **36**, 531–537 (1995).
42. L’Episcopo, F. *et al.* Wnt/beta-catenin signaling is required to rescue midbrain dopaminergic progenitors and promote neurorepair in ageing mouse model of Parkinson’s disease. *Stem Cells*, doi:10.1002/stem.1708 (2014).
43. Siddiqi, S. & Sussman, M. A. Cardiac Hegemony of Senescence. *Curr Transl Geriatr Exp Gerontol Rep* **2**, doi:10.1007/s13670-013-0064-3 (2013).
44. Cieslik, K. A., Trial, J., Crawford, J. R., Taffet, G. E. & Entman, M. L. Adverse fibrosis in the aging heart depends on signaling between myeloid and mesenchymal cells; role of inflammatory fibroblasts. *J Mol Cell Cardiol* **70C**, 56–63, doi:10.1016/j.yjmcc.2013.10.017 (2014).
45. Goichberg, P. *et al.* Age-associated defects in EphA2 signaling impair the migration of human cardiac progenitor cells. *Circulation* **128**, 2211–2223, doi:10.1161/CIRCULATIONAHA.113.004698 (2013).
46. Despars, G., Carbonneau, C. L., Bardeau, P., Coutu, D. L. & Beausejour, C. M. Loss of the osteogenic differentiation potential during senescence is limited to bone progenitor cells and is dependent on p53. *PLoS One* **8**, e73206, doi:10.1371/journal.pone.0073206 (2013).
47. Ting, C. H., Ho, P. J. & Yen, B. L. Age-related decreases of serum-response factor levels in human mesenchymal stem cells are involved in skeletal muscle differentiation and engraftment capacity. *Stem Cells Dev* **23**, 1206–1216, doi:10.1089/scd.2013.0231 (2014).
48. Marschallinger, J. *et al.* Age-dependent and differential effects of Smad7DeltaEx1 on neural progenitor cell proliferation and on neurogenesis. *Exp Gerontol* **57**, 149–54, doi:10.1016/j.exger.2014.05.011 (2014).
49. Bouab, M., Paliouras, G. N., Aumont, A., Forest-Berard, K. & Fernandes, K. J. Aging of the subventricular zone neural stem cell niche: evidence for quiescence-associated changes between early and mid-adulthood. *Neuroscience* **173**, 135–149, doi:10.1016/j.neuroscience.2010.11.032 (2011).
50. Behrens, A., van Deursen, J. M., Rudolph, K. L. & Schumacher, B. Impact of genomic damage and ageing on stem cell function. *Nat Cell Biol* **16**, 201–207, doi:10.1038/ncb2928 (2014).
51. Lee, P. J., Hung, P. J., Rao, V. M. & Lee, L. P. Nanoliter scale microbio-reactor array for quantitative cell biology. *Biotechnol Bioeng* **94**, 5–14, doi:10.1002/bit.20745 (2006).
52. Ottesen, E. A., Hong, J. W., Quake, S. R. & Leadbetter, J. R. Microfluidic digital PCR enables multigene analysis of individual environmental bacteria. *Science* **314**, 1464–1467, doi:10.1126/science.1131370 (2006).
53. Whitesides, G. M. The origins and the future of microfluidics. *Nature* **442**, 368–373, doi:10.1038/nature05058 (2006).
54. Levi, B. *et al.* Molecular analysis and differentiation capacity of adipose-derived stem cells from lymphedema tissue. *Plast Reconstr Surg* **132**, 580–589, doi:10.1097/PRS.0b013e31829ace13 (2013).
55. Levi, B. *et al.* CD105 protein depletion enhances human adipose-derived stromal cell osteogenesis through reduction of transforming growth factor beta1 (TGF-beta1) signaling. *J Biol Chem* **286**, 39497–39509, doi:10.1074/jbc.M111.256529 (2011).
56. Suga, H. *et al.* Tracking the elusive fibrocyte: Identification and characterization of collagen producing hematopoietic lineage cells during murine wound healing. *Stem Cells* **32**, 1347–60, doi:10.1002/stem.1648 (2014).
57. Sawada, H. *et al.* Reduced BMP2 expression induces GM-CSF translation and macrophage recruitment in humans and mice to exacerbate pulmonary hypertension. *J Exp Med* **211**, 263–280, doi:10.1084/jem.20111741 (2014).
58. Pandey, A. C. *et al.* MicroRNA profiling reveals age-dependent differential expression of nuclear factor kappaB and mitogen-activated protein kinase in adipose and bone marrow-derived human mesenchymal stem cells. *Stem Cell Res Ther* **2**, 49, doi:10.1186/srct90 (2011).
59. Blackburn, E. H. Telomerase and Cancer: Kirk A. Landon--AACR prize for basic cancer research lecture. *Mol Cancer Res* **3**, 477–482, doi:10.1158/1541-7786.MCR-05-0147 (2005).
60. Chen, D. *et al.* Germline signaling mediates the synergistically prolonged longevity produced by double mutations in daf-2 and rsk-1 in *C. elegans*. *Cell Rep* **5**, 1600–1610, doi:10.1016/j.celrep.2013.11.018 (2013).

Acknowledgements

The authors would like to thank Yujin Park for her assistance with tissue processing and staining. Flow cytometric analyses for this manuscript were completed at the Stanford Shared FACS Facility. Funding for the stem cell research conducted in our laboratory has been provided by the Hagey Family Endowed Fund in Stem Cell Research and Regenerative Medicine, the Armed Forces Institute of Regenerative Medicine (United States Department of Defense), the National Institutes of Health (R01-DK074095, R01-EB005718, R01-AG025016 to G.C.G. and T35-HL007479 to E.A.), and the Oak Foundation.

Author contributions

All listed authors contributed to the idea generation, design, and completion of this work. D.D., R.C.R. and M.J. contributed equally to the idea generation, experimental work and manuscript preparation. E.A., Z.N.M., A.J.W., M.G.P., R.K., M.S.H., G.G.W., D.A. and S.K. contributed to the experimental work and manuscript preparation. A.J.B. and G.C.G. guided the idea generation, experimental work and manuscript preparation.

Additional information

Supplementary information accompanies this paper at <http://www.nature.com/scientificreports>

Competing financial interests: Yes, there is potential Competing Interest. D.D., R.C.R. and G.C.G. are listed on the patent “Efficient stem cell delivery into biomaterials using a novel capillary driven encapsulation technique” and G.C.G. is listed on the patent “Intelligent Biodegradable Pullulan Regenerative Matrix for Tissue Engineering” assigned to Stanford University. M.J., E.A., Z.N.M., A.J.W., M.G.P., R.K., M.S.H., G.G.W., D.A., S.K. and A.J.B. have no potential conflicts of interest, affiliations or financial involvement with any organization or entity with a financial interest in or financial conflict with the subject matter or materials discussed herein.

How to cite this article: Duscher, D. *et al.* Aging disrupts cell subpopulation dynamics and diminishes the function of mesenchymal stem cells. *Sci. Rep.* **4**, 7144; DOI:10.1038/srep07144 (2014).



This work is licensed under a Creative Commons Attribution-NonCommercial-NoDerivs 4.0 International License. The images or other third party material in this article are included in the article’s Creative Commons license, unless indicated otherwise in the credit line; if the material is not included under the Creative Commons license, users will need to obtain permission from the license holder in order to reproduce the material. To view a copy of this license, visit <http://creativecommons.org/licenses/by-nc-nd/4.0/>